The spectra characteristic of capacitive virtual Frisch grid detectors with different directions

ZHUBIN SHI, LINJUN WANG[*], KAIFENG QIN, JIAHUA MIN, JIJUN ZHANG, XIAOYAN LIANG, JIAN HUANG, KE TANG, YIBEN XIA
School of Materials Science and Engineering, Shanghai University, Shanghai 200072, China

Recent years, CdZnTe detectors have captured great interests in the field of gamma ray detection for their special characteristics. The configuration of virtual Frisch grid detector has better charge collection efficiency (CCE) than normal planar detector. In our study we introduce capacitive virtual Frisch grid structure and Schottky contact to further reduce the leakage current which can be confirmed in current-voltage (I-V) curves. The spectra response of the different directions in capacitive virtual Frisch grid CdZnTe detectors seem subtle different and independent of both material characteristics and fabricating process, furthermore their trends have been obtained. The primary results show that it is possible to detect the both directions of the radioactive source and radioisotope in hand-held gamma-ray instruments. More experiments need to do in the wide range of CdZnTe material and various radioactive sources to clear these results.

1. Introduction

Recently, CdZnTe crystals which have the characteristic of wide bandgap, high resistivity and high atomic number, have been developed rapidly for the fabrication of nuclear radiation detectors in the fields of X-ray and gamma ray detection, nuclear physics and nuclear medicine [1-3]. Compared to the binary compound CdTe, the ternary compound CdZnTe is more promising for room temperature radiation detectors because the addition of Zn to CdTe results in an increased band gap as well as the energy of defect formation, and overcomes the polarization effect of CdTe, which limits the exploitation of CdTe detectors [3].

Unfortunately, after so many years of material research and development, the transport properties of the carriers in CdZnTe, especially the low holes mobility-lifetime product $(\mu\tau)_h$, reduce the charge collection efficiency (CCE) of the detectors and produce an asymmetric long holes tail in the photopeaks of the measured spectra. These poor transport properties of the carriers in CdZnTe limit both the size and energy resolution of detectors [4-6]. And an important characteristic of gamma-ray spectrometer is the uniformity of response to gamma ray, which means the pulse height response is constant for any given energy deposited in the detector and is not dependent upon the location where the gamma ray is absorbed [7]. Nowadays, several irradiation configurations of the detectors [8], such as virtual Frisch grid device, pixilated device and co-planar device, have been developed to minimize this effect and provide good quality spectra. Besides, advanced charge carrier sensing techniques, such as pulse rise-time discrimination and

bi-parametric analysis [9], have been exploited to decrease the holes tailing effect.

Note that the virtual Frisch grid detector with a shielding electrode (extended cathode), unlike many other single carrier device designs, offers excellent spectroscopic performance at the lowest cost without any complicated read-out electronics and digital or electronic corrections [1,2,3,7]. The shape of the virtual Frisch grid device makes it ideal building blocks for assembling large arrays, which provides large effective area, good energy resolution and spatial resolution at comparatively low production cost. In this paper, the capacitive virtual Frisch grid CdZnTe device is designed with a Schottky and ohmic contact on each of the two sides of CdZnTe wafer, which further reduces the leakage current even with a high bias voltage and realizes good energy resolution in identifying the radioisotope. Meanwhile, since the radiation hand-held dosimeters can only measure the radiation dose and determine the radioisotope, but they cannot point out the direction of the radiation sourcing [10], which limit their usage in the nuclear security fields. In this work, the spectra response of different directions for capacitive virtual Frisch grid CdZnTe detectors was acquired, which can be used to obtain the directional information in the next generation of nuclear detector.

2. Theoretical consideration and detector design

It is known to all that the CCE of nuclear detector depends on the charge carrier transport properties of a device (the mobility and mean lifetime of electrons and

holes, such as $\mu_{e,h}$ or $\tau_{e,h}$, respectively), weighting potential, and the applied electric fields [7, 8, 11, 12]. The initially generated charge pairs are swept from the interaction region by the effect of applied bias (V) towards the opposite potential electrodes. Electrons drifted to the positive electric field electrode (anode) and holes drifted to the negative electric field (cathode). However, some trapping will occur in the trajectory of carriers' movement. So the velocity of the charge carriers is generally defined as

$$v_{e,h}(x) = \mu_{e,h}\frac{dV(x)}{dx} = \mu_{e,h}E(x) \qquad (1)$$

where E is the local electric field with respect to position x. Charge trapping is typically modeled as a function of time. The total number of free charge carriers $N(t)$ remaining in motion at time t is [8].

$$N(t) = N_0\exp\left[-\frac{t}{\tau_e}\right] + N_0\exp\left[-\frac{t}{\tau_h}\right] \quad t = \frac{x}{v} = \frac{x}{\mu_{e,h}E(x)} \quad (2)$$

where $N_0 (= \frac{E_\gamma}{w})$ is the charge generated in a photoelectric event in a CdZnTe device, E_γ is the gamma-ray energy, w is the average ionization energy for CdZnTe. To determine the operating potential V, Poisson's equation must be solved with the appropriate boundary conditions

$$\nabla(\nabla V) = -\frac{\rho}{\varepsilon_0\varepsilon_s} \qquad (3)$$

where ε_0 is the permittivity of vacuum, V is the applied voltage potential, ρ is the space charge within the semiconductor, and ε_s is the dielectric constant of the material. The boundary conditions are such that all electrodes are at their respective potentials where the collecting electrode (anode) is biased and the non-collecting electrode (cathode) is grounded. The weighting potential is calculated under the condition that all space charges are removed, so the weighting potential φ_W in a device is found by solving the Laplace equation form Eq. 2.3

$$\nabla(\nabla\varphi_W) = \frac{0}{\varepsilon_0\varepsilon_s} = 0 \qquad \nabla(\varepsilon_s\varepsilon_0\nabla\varphi_W) = 0 \qquad (4)$$

The Shockley-Ramo Theorem states that the change of the induced charge ΔQ_L on an electrode **L** by the movement of charge q from position x_i to position x_f is

$$\Delta Q_L = \int_{x_i}^{x_f} i(t)dt = \int_{x_i}^{x_f} qN(t)E_0 dx = \int_{x_i}^{x_f} qN(t)d\varphi_W = -qN_{avg}\left[\varphi_0(x_f) - \varphi_0(x_i)\right]$$

$$(5)$$

where q is the elementary charge of the carriers, $N(t)$ is the instantaneous number of free charge carriers, and φ_W is the weighting potential through which the charge carrier is moving, N_{avg} is the average number of free charge carriers over time step t.

Therefore, charge collection is determined by two step fundamental quantities, the number of charge carriers and the change in weighting potential through which they move, which means the induced charge on electrode L is only determined by the starting and stopping positions of the charge carriers, and is independent of the actual electric field and the space charges.

So the CCE for a virtual Frisch grid detector with charge trapping, assuming uniform material and electric field and neglecting de-trapping, is described by the Hecht equation [11]

$$CCE_{th} = \frac{E\mu_e\tau_e}{d}\left[1 - \exp\left(-\frac{x}{E\mu_e\tau_e}\right)\right] + \frac{E\mu_h\tau_h}{d}\left[1 - \exp\left(-\frac{(d-x)}{E\mu_h\tau_h}\right)\right]$$

$$(6)$$

where d is the detector thickness, x is depth from cathode in the detector, E is the electric field applied to the detector, $\mu_{e(h)}$ is the mobility of electrons (holes), $\tau_{e(h)}$ is the mean lifetime of carriers for electrons (holes).

The general configuration of a capacitive virtual Frisch grid CdZnTe detector is designed and shown in Fig. 1. The area of the extended cathode is the interaction region (d_i) and the area between the anode and the extended cathode is the collection region (d_c). As previously discussed, although the electric field is not constant in practice and theory, it is assumed constant for simplicity near the cathode and the shielding (grounded) and rises rapidly close to the anode (biased), and the assumption on constant electric field will not change the simulation and prediction significantly. Then if the incident gamma photon interacted in the interaction region, then only electron will contributed to the induced charge because the weighting potential for holes is constant. Taking the trapping effect into consideration and neglecting the correction factor for deviations in the weighting potential, the induced charge from electrons excited in the interaction region by a gamma ray event at a distance x_i from the cathode will be [12]

$$CCE = \frac{Q^*}{Q_0} = \frac{E\mu_e\tau_e}{d_c}\left(1 - \exp\left[-\frac{d_i}{E\mu_e\tau_e}\right]\right)\exp\left[\frac{x_i - d_i}{E\mu_e\tau_e}\right] \quad (7)$$

where d_c, d_i is the length of the collection and interaction region respectively.

For gamma ray interactions that occur directly in the collection region, the induced charge will now be dependent on both electrons and holes motion within the collection region. Taking the trapping effect into

consideration and neglecting the correction factor for deviations in the weighting potential, the induced charge from gamma ray events occurring in the collection region is [12]

$$CCE = \frac{Q^*}{Q_0} = \frac{E\mu_e\tau_e}{d_c}\left(1-\exp\left[\frac{x_i-d}{E\mu_e\tau_e}\right]\right) + k(x,y)\frac{E\mu_h\tau_h}{d_c}\left(1-\exp\left[\frac{d_i-x_i}{E\mu_h\tau_h}\right]\right) \quad (8)$$

Fig. 2 shows the plots of CCE for a planar detector and a capacitive virtual Frisch grid detector according to equations 2.6~2.8, where supposes the $\tau_e = 4\mu s, \tau_h = 100ns, \mu_e = 1350cm^2/Vs, \mu_h = 120cm^2/Vs$, and E=1.2×10⁵V/m. It's found that the CCE rises slowly from 86.36% at cathode to about 99% at the edge of the extended cathode in virtual Frisch grid detector. The reason for this phenomenon is that the effect of trapping will occur when electrons sweep to the anode while the trapping probability at the edge of the extended cathode can be neglected for the collection region is much less than the mean free length of electrons. Then the CCE drops significantly from about 99% at the edge of the extended cathode to about 14% at the anode. This is because, in the anode, the holes are contributed to the induced charges besides the electrons. It can be apparently seen that the CCE for virtual Frisch grid detector is much bigger than that of planar one. Therefore the virtual Frisch grid detector was fabricated in our research.

Fig. 1. The configuration of capacitive virtual Frisch grid CdZnTe detector.

Fig. 2. Theoretically predicted curves of the CCE of capacitive virtual Frisch grid CdZnTe detector and planar detector

3. Experimental

The CdZnTe single crystal was prepared by the modified low-pressure vertical Bridgman method under Te-rich conditions with high purity raw materials Cd (7N), Zn (7N), Te (7N) and In (7N) [13, 14]. The configuration of the capacitive virtual Frisch grid detector in this design is different from normal ones, which has a dielectric material covering the almost entire region more than the shielding electrodes between the anode and the cathode electrodes. The four sides of CdZnTe wafers were hand polished and etched briefly with a 5 vol% bromine/methanol solution and a 2 vol% bromine/20 vol% Lactic acid/ethylene glycol solution. The metal contacts were deposited on the two opposite sides of CdZnTe wafers to form the anode and cathode. As the conductivity characteristic of the as-grown CdZnTe material is P-type, In was used to form the Schottky contact by physical vapor deposition and Au was used to fabricate ohmic contact by chemical deposition [15~17]. Afterwards, CdZnTe wafers were treated by a two-step chemical passivation process with KOH-KCL/NH₄F-H₂O₂ solution [18] to reduce side-surface leakage current and improve the performance. Finally, the CdZnTe wafers were wrapped in Teflon tape and copper foil (which were grounded at cathode). A schematic design of the capacitive virtual Frisch grid CdZnTe detector is shown in Figure 1 [19]. The CdZnTe detector is with the dimension of $10\times10\times10mm^3$, while the insulation layer is 0.95mm, the thickness of the insulation layer and the copper tape is 0.2 mm and the length of the copper shims (d_i) is 0.9 mm. Four CdZnTe detectors, designated as A, B, C and D, were fabricated according to the above steps from the middle position of an ingot. Gold pogo-pins were bonded to the anode and cathode with conductive epoxy, which was used to connect to the bias voltage (1200 V) and preamplifier.

During the spectra response to Gamma-ray measurements, the CdZnTe detector was placed in an aluminum electronics box and the output of electrons in the anode to the preamplifier was connected by a BNK jack. The spectra responses of different Gamma-ray directions for capacitive virtual Frisch grid CdZnTe detectors were acquired. The operational principle is based on the difference of charge carrier trapping in CZT crystal. The incident angle of Gamma-ray was changed from 0 to 180 degree. The schematic of the incident angle and the relative position of radioactive source to detector are shown in Figure 3. The radioactive source is uncollimator ¹³⁷Cs which is 80 cm away from detector, and the radioactive source is always at same direction no matter how the central axis of detectors changes, which is shown in Fig. 3. Signals from detectors before being sent to the multi-channel were processed through a preamplifier and a shaping amplifier respectively, which was discussed elsewhere [20].
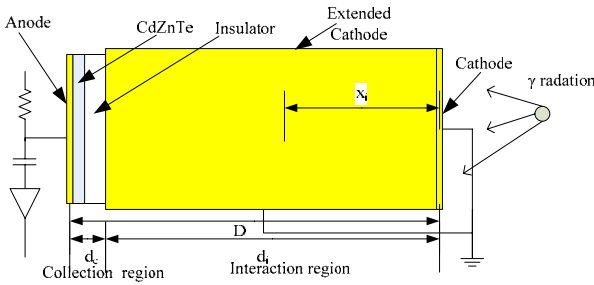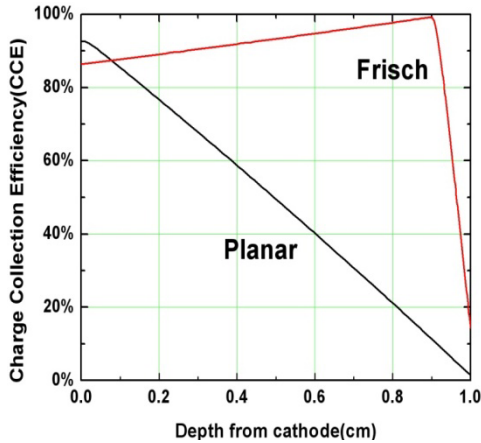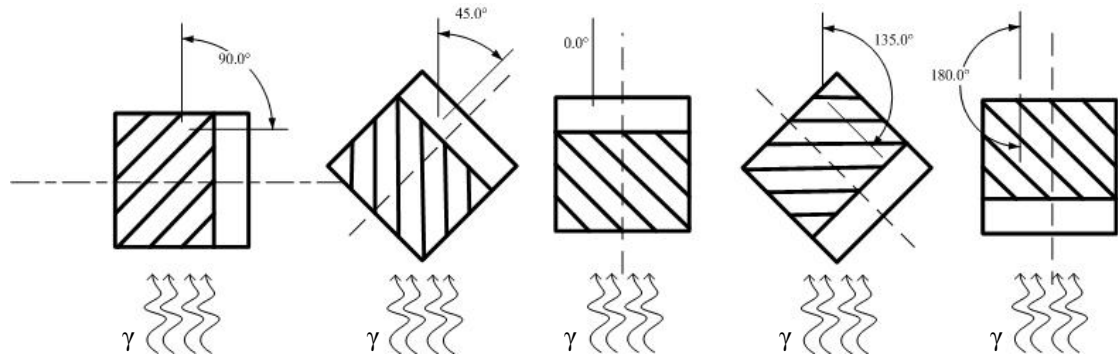
Fig. 3. The diagram of the changed incident angle from 0 to 180 degree.

4. Results and discussion

Fig. 4 indicates the four *I-V* curves of the four In/p-CZT/Au detectors, respectively. These four curves show good rectifying effect and Schottky contact which reduce the leakage current. But there exists some divergence because the four CdZnTe wafers were cut from the different positions of the same ingot. The crystal nucleus of the ingot is not uniform and distributed randomly. It should be noted that there exists a wide range of holes lifetime due to trapping defects from one detector to another, which is not well controlled by current manufacturing practices and can easily vary over an order of magnitude. Since the spectra responses of different Gamma-ray directions do not depend on the material characteristics or fabricating processes, which will be shown as below, however the slight differences in current variations of I-V curves in CdZnTe detectors relevant to material properties will be explained in another paper.
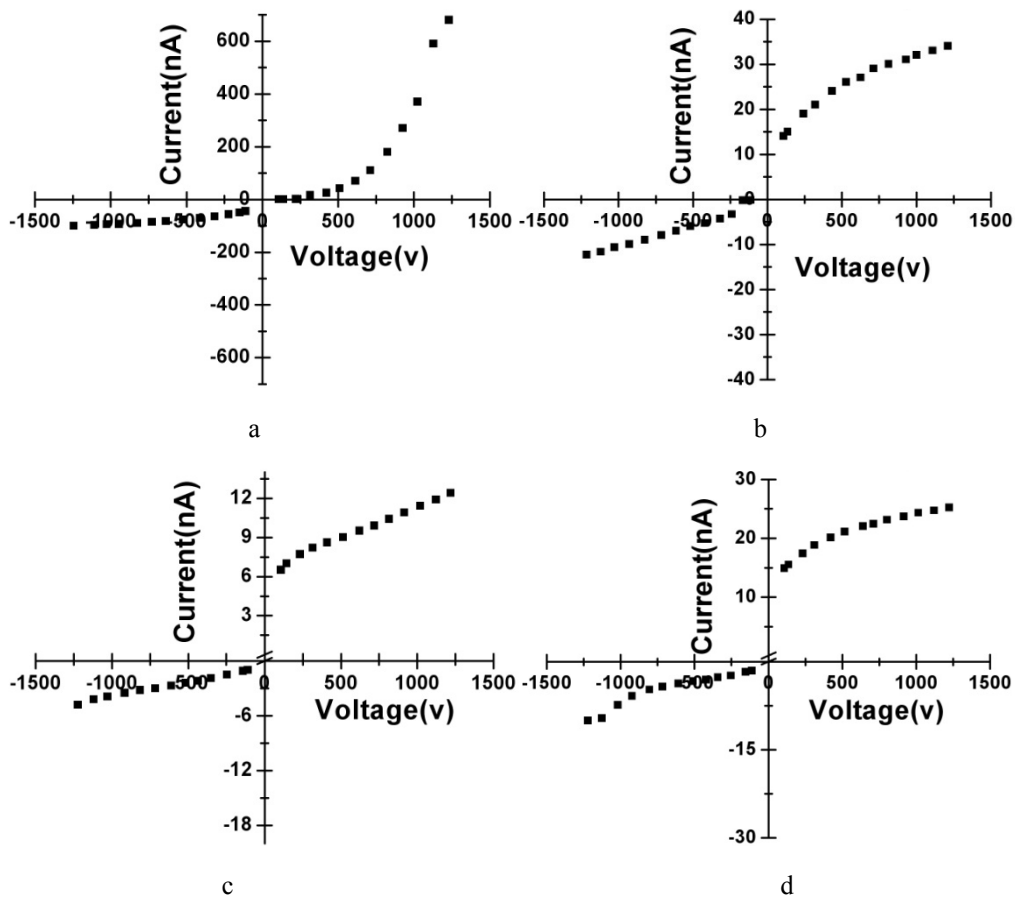

Fig. 4. I-V characteristics of detector A, B, C and D showed in (a), (b), (c) and (d) respectively.

Fig. 5 shows the spectra responses of different gamma-ray directions on devices A, B, C and D. The photoelectric peak, Compton plate and backscattering peak can be determined apparently. In Figure 5 it is hard to distinguish the subtle differences between 45˚ and 90˚ directions in all the response spectra for detector A, B, C or D. So some parameters are used to mark the distinctions such as the peak to Compton ration (PTCR), the full width at half maximum (FWHM) and photo peak. A brief discussion of these characteristics follows.
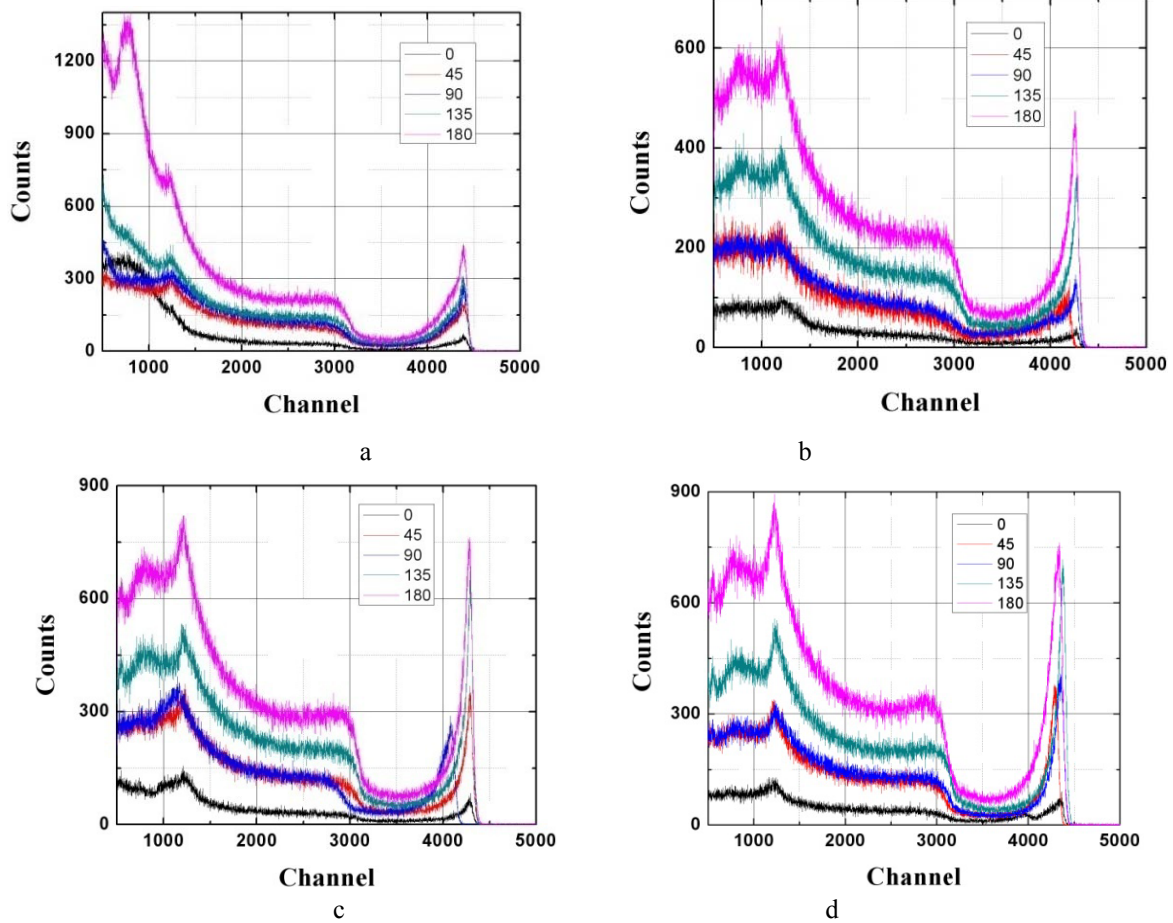

Fig. 5. the spectra responses of different directions of devices A, B, C and D showed in (a), (b), (c) and (d) respectively.

The peak to Compton ration (PTCR) is determined by dividing the counts per channel of photo peak over average counts per channel of flat Compton plateau. In order to simplify the calculation, the energy range of backscattering peak to photoelectric peak is used. The ration is typically a measure of the combined effects of detector energy resolution and the energy absorptivity of an incoming gamma ray. The PTCR of four detectors is shown in Figure 6. It can be seen that the PTCR rose gradually from 0 degree to 135 degree, but dropped rapidly at 180 degree. The full width at half maximum (FWHM) of the spectra response is applied to represent the resolution of CdZnTe detector. The FWHM values decrease from 0˚ to 135˚ and increase from 135˚ to 180˚, which means the Gamma-ray direction of 135˚ has the best energy resolution and is shown in Figure 7. The photo peak is determined by the photoelectric peak channel, which is proportional to the output amplitude of signal from the charge sensitive preamplifier. Fig. 8 indicates that the largest amplitude of signal is at the incident angle of 135˚, even though the CdZnTe wafers may have various crystalline properties and fabrication process.
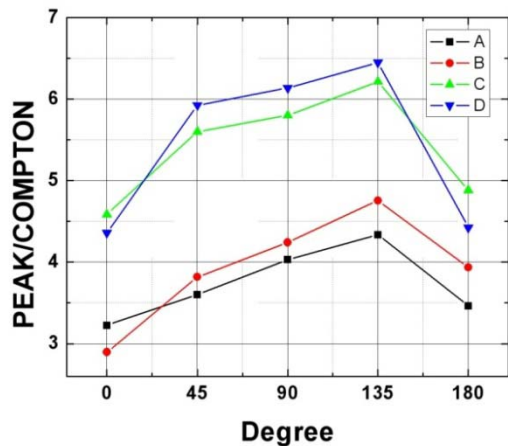

Fig. 6. Peak to Compton ration (PTCR) at different incident angles of Gamma-ray with detector A, B, C and D.
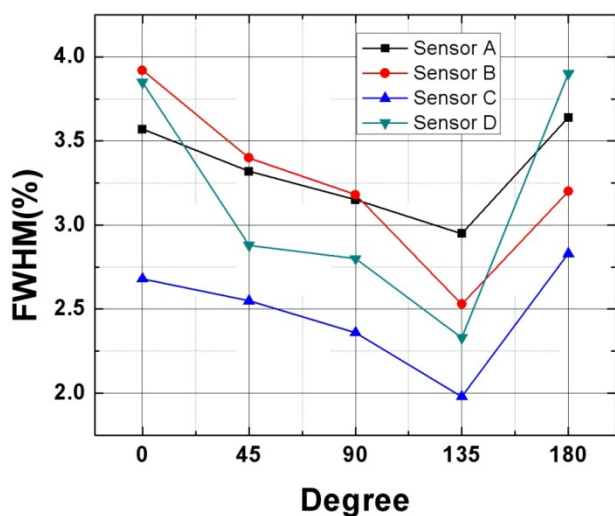
Fig. 7. The FWHM at different incident angles of Gamma-ray with detectors A, B, C and D
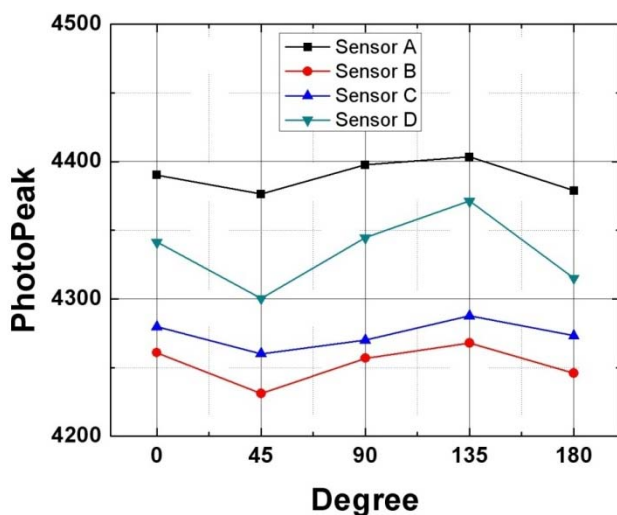

Fig. 8. The photo peak channel at different incident angles of Gamma-ray with detectors A, B, C and D.

It is noted that the entire variation trend of PTCR, FWHM and photopeak in the energy spectra of virtual Frisch grid CdZnTe detectors is the same. The gamma-ray direction of 135˚ seems to have the best performance among all directions. The results show that to detect the direction of the radioactive source and determine the radioisotope simultaneously is feasible. The design and fabrication of such portable instrument of capacitive virtual Frisch grid detector is underway.

5. Conclusion

In this work, the capacitive virtual Frisch grid configuration of CdZnTe detectors was fabricated and their spectra response of various gamma-ray directions was acquired. The CCE for virtual Frisch grid detector was calculated. The spectra response of different directions of capacitive virtual Frisch grid CdZnTe detectors shows different and has its variation trend, so the direction of radioactive source can be determined by comparing the spectra obtained by changing the direction of the detector, which has great meaning for hand-held radioisotope and direction identifier.

References

[1] W. J. McNeil, D.S. McGregor, A. E. Bolotnikov et al., Appl. Phys. Lett., **84**, 1988 (2004).
[2] G. W. Wright, G. Camard, E. Kakuno et al., Proc. SPIE, **5198**, 306 (2004).
[3] A. E. Bolotnikov, G. C. Camarda, G. A. Carini et al., Performance Characteristics of Frisch-Ring CdZnTe Detectors, IEEE Transactions on Nuclear Science, **53**, No. 2, (2006).
[4] A.E. Bolotnikov, G.S. Camarda, G.A. Carini, et al, Nucl. Instrum. Methods Phys. Res. A **579**, 125 (2007).
[5] K.H. Kim, R. Gul, V. Carcelen, et al, J. Crystal Growth, **312**, 781 (2010).
[6] Yang, Ge, Wanqi Jie, et al., Journal of Crystal Growth, **283**(3-4), 431 (2005).
[7] Alireza Kargar, Mark J. Harrison, Adam C. et al., Nuclear Instruments and Methods in Physics Research A **620** 270 (2010).
[8] Mark J. Harrison, Alireza Kargar, Douglas S. McGregor et al., Charge collection characteristics of Frisch collar CdZnTe gamma-ray spectrometers, Nuclear Instruments and Methods in Physics Research A **579**, 134 (2007).
[9] N. Auricchio, L. Amati, A. Basili et al., IEEE Trans. Nucl. Sci. **52**, 1982 (2005).
[10] Se-Hwan Park, Nam-Ho Lee, S.M. Lee et al., Applied Radiation and Isotopes, **67**, 1471 (2009).
[11] R. Redus, A. Huber, J. Pantazis et al., IEEE Transactions on Nuclear Science, **51**(5), (2004).
[12] D.S McGregor, Z. He, H.A. Seifert et al., IEEE Transactions on Nuclear Science **45**, No. 3, (1998).
[13] T.E. Schlesinger, J.E. Toney, H. Yoon et al., Mater. Sci. Eng..**32**(4-5), 103 (2001).
[14] A. Burger, M. Groza, Y. Cui et al., Phys. Status Solidi, **2**(5), 1586 (2005).

[15] Shin Hang Cho, Jong Hee Suh and Jae Ho Won et al, Nuclear Instruments and Methods in Physics Research A **591**, 203 (2008).

[16] Jae Ho Won, Ki Hyun Kim, Jong Hee Suh et al., Nuclear Instruments and Methods in Physics Research A **591,** 206 (2008).

[17] KiHyun Kim, ShinHang Cho and JongHee Suh et al., Schottky-type polycrystalline CdZnTe X-ray detectors, Current Applied Physics **9,** 306 (2009).

[18] D.S. McGregor, US Patent no. 6,781,132, August 24, 2004.

[19] Sang Wenbin, Wang Kunshu and Min Jiahua et al., Semicond. Sci. Tech. **20,** 343 (2005).

[20] Zhubin Shi, Wenbin Sang, Yongbiao Qian, et.al, Readout and Signal Processing Electronics for 2*2 CZT Detectors in Parallel, The 9th International Conference on Solid-State and Integrated- Circuit Technology 2008, 992-995.

*Corresponding author: ljwang@shu.edu.cn